

The Probable Fate of the Standard Model

J. Ellis^a, J.R. Espinosa^{a,b}, G.F. Giudice^a, A. Hoecker^a and A. Riotto^{a,c}

^a*Physics Department, CERN, CH-1211 Geneva 23, Switzerland*

^b*ICREA, Institució Catalana de Recerca i Estudis Avançats,*

at IFAE, Universitat Autònoma de Barcelona, 08193 Bellaterra, Barcelona, Spain

^c*INFN, Sezione di Padova, Via Marzolo 8, I-35131 Padua, Italy*

Abstract

Extrapolating the Standard Model to high scales using the renormalisation group, three possibilities arise, depending on the mass of the Higgs boson: if the Higgs mass is large enough the Higgs self-coupling may blow up, entailing some new non-perturbative dynamics; if the Higgs mass is small the effective potential of the Standard Model may reveal an instability; or the Standard Model may survive all the way to the Planck scale for an intermediate range of Higgs masses. This latter case does not necessarily require stability at all times, but includes the possibility of a metastable vacuum which has not yet decayed. We evaluate the relative likelihoods of these possibilities, on the basis of a global fit to the Standard Model made using the Gfitter package. This uses the information about the Higgs mass available directly from Higgs searches at LEP and now the Tevatron, and indirectly from precision electroweak data. We find that the ‘blow-up’ scenario is disfavoured at the 99% confidence level (96% without the Tevatron exclusion), whereas the ‘survival’ and possible ‘metastable’ scenarios remain plausible. A future measurement of the mass of the Higgs boson could reveal the fate of the Standard Model.

1 Introduction

The success of the Standard Model (SM) offers very few experimental clues how it may break down, and at what scale. One clue is provided by the discovery of neutrino masses, which suggest the appearance of new physics at a mass scale of a TeV or more, probably at least 10^{10} GeV in the simplest versions of seesaw models. Another clue might be offered by the measurement of the anomalous magnetic moment of the muon, if one could be sure of the value within the SM. However, this requires input from data on low-energy e^+e^- annihilation and/or τ decay into hadrons about which there is, unfortunately, as yet no consensus. The existence of dark matter could be another clue to physics beyond the SM, assuming it does not have some astrophysical origin such as primordial black holes. The baryon asymmetry of the Universe can also be explained only by physics beyond the SM, which could appear anywhere between the electroweak and inflation scales.

In view of this paucity of experimental hints about possible physics beyond the SM, any new indications would be most welcome. We discuss in this paper the one important hint about the possible scale of new physics that may (soon) be provided by the Higgs sector of the SM. There are, of course, plenty of theoretical arguments why the Higgs sector of the SM is inadequate, many of them related to the apparently unnatural fine-tuning of its parameters, but we have in mind a more direct empirical argument based on the available experimental information about the Higgs sector.

The most direct information comes from experimental searches for the SM Higgs boson, first at LEP and more recently at the Tevatron. These exclude a Higgs mass $M_H < 114.4$ GeV [1] and between 160 and 170 GeV [2] at the 95% confidence level (CL), and also provide contributions to the overall SM likelihood function for other values of the Higgs mass. Another contribution to the Higgs likelihood function comes from a global fit to electroweak precision data within the SM, which favours $M_H < 158$ GeV [3] (95% CL, not including the direct Higgs searches). Figure 1 shows the $\Delta\chi^2$ function obtained from the global fit without (left hand plot) and with (right) the information from the direct Higgs searches at LEP and the Tevatron.

It is well known that the Higgs sector of the SM must steer a narrow course between two problematic situations if it is to survive up to the reduced Planck scale $M_P \sim 2 \times 10^{18}$ GeV, by which some new physics associated with quantum gravity must surely appear [4, 5, 6, 7, 8]. If M_H is large enough, the renormalisation-group equations (RGEs) of the SM drive the Higgs self-coupling into the non-perturbative regime at some scale $\Lambda < M_P$, entailing either new non-perturbative physics at a scale $\sim \Lambda$, or new physics at some scale $< \Lambda$ that prevents

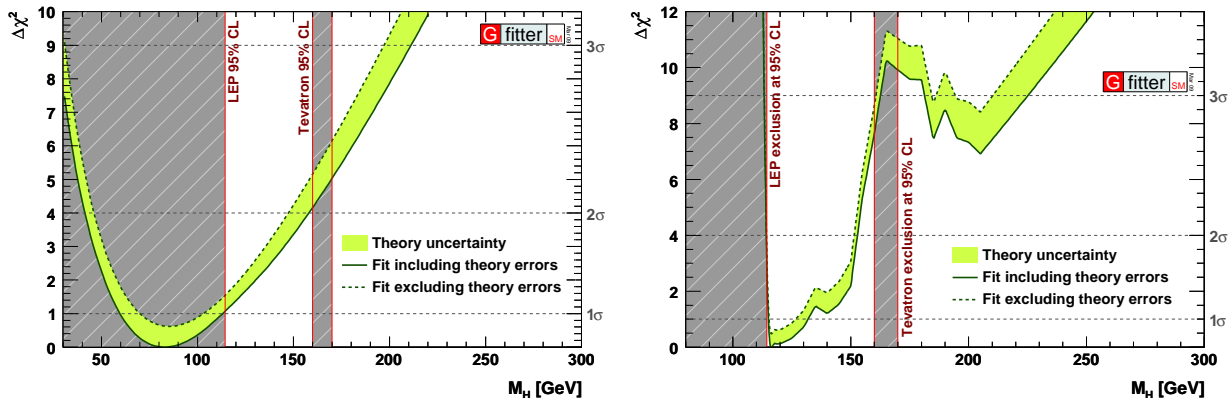


Figure 1: *Dependence on M_H of the $\Delta\chi^2$ function obtained from the global fit of the SM parameters to precision electroweak data [3], excluding (left) or including (right) the results from direct searches at LEP and the Tevatron.*

the Higgs self-coupling from blowing up. This is shown as the upper pair of bold [blue] lines in Fig. 2. On the other hand, if M_H is small enough, the RGEs drive the Higgs self-coupling to a negative value at some Higgs field value $\Lambda < M_P$, in which case the electroweak vacuum is only a local minimum and there is a new, deep and potentially dangerous minimum at scales $> \Lambda$. The electroweak vacuum can potentially become unstable against collapse (either because of zero-temperature (quantum) or thermal tunneling during the evolution of the universe) into that deeper new vacuum with Higgs vacuum expectation value $> \Lambda$, unless there is new physics at some scale $< \Lambda$ that prevents the appearance of that vacuum. This is shown, with its uncertainties, as the light shaded [green] bands in Figs. 2 and 3. Below this stability bound, there is a region we dub the ‘metastability’ region where the electroweak vacuum has a lifetime longer than the age of the Universe for decay via either zero-temperature quantum fluctuations (region above the dark shaded [red] bands in these figures) or thermal fluctuations (region above the medium shaded [blue] bands). Between the ‘blow-up’ and ‘metastability’ cases, there is a range of intermediate values of M_H for which the SM could survive up to the Planck scale.

In this paper we update and complete previous calculations of these bounds on M_H , and then make quantitative estimates of the relative likelihoods of these ‘blow-up’, ‘collapse’, ‘metastable’ and ‘survival’ scenarios, on the basis of a combined analysis of the information currently available about the possible mass of the Higgs boson within the SM, including both experimental and theoretical uncertainties. Our principal conclusion is that the non-perturbative ‘blow-up’ scenario is now disfavoured at the 99.1% CL after inclusion of the recent Tevatron exclusion of a SM Higgs boson weighing between 160 and 170 GeV [2], whereas this scenario could only have been excluded at the 95.7% CL if the Tevatron infor-

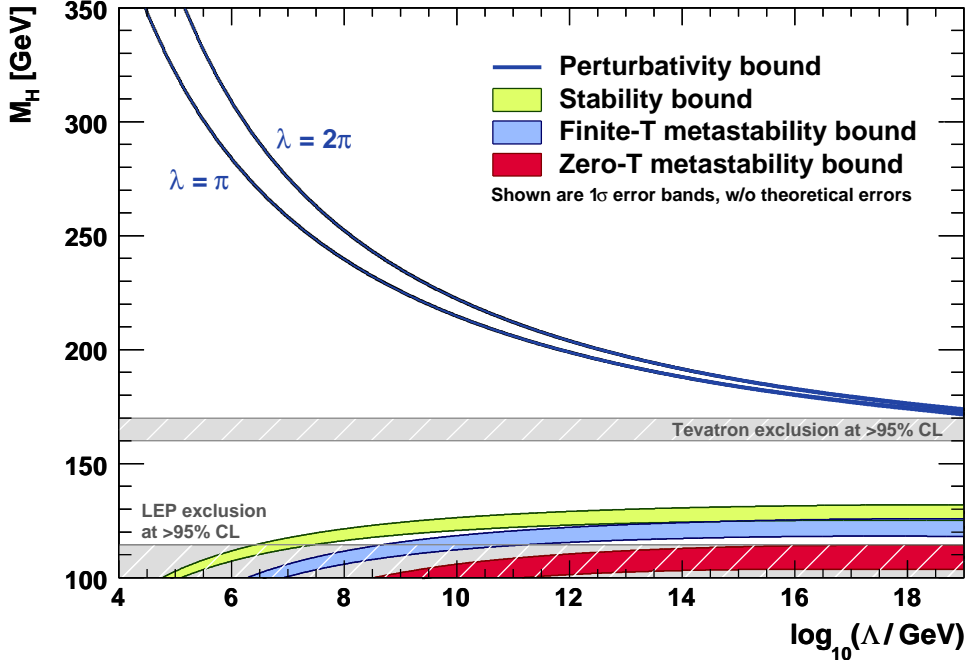


Figure 2: The scale Λ at which the two-loop RGEs drive the quartic SM Higgs coupling non-perturbative, and the scale Λ at which the RGEs create an instability in the electroweak vacuum ($\lambda < 0$). The width of the bands indicates the errors induced by the uncertainties in m_t and α_s (added quadratically). The perturbativity upper bound (sometimes referred to as ‘triviality’ bound) is given for $\lambda = \pi$ (lower bold line [blue]) and $\lambda = 2\pi$ (upper bold line [blue]). Their difference indicates the size of the theoretical uncertainty in this bound. The absolute vacuum stability bound is displayed by the light shaded [green] band, while the less restrictive finite-temperature and zero-temperature metastability bounds are medium [blue] and dark shaded [red], respectively. The theoretical uncertainties in these bounds have been ignored in the plot, but are shown in Fig. 3 (right panel). The grey hatched areas indicate the LEP [1] and Tevatron [2] exclusion domains.

mation were not included. On the other hand, the Tevatron data, although able to narrow down the region of the ‘survival’ scenario, have no significant impact on the relative likelihoods of the ‘collapse’, ‘metastable’ and ‘survival’ scenarios, neither of which can be excluded at the present time.

We also consider the prospects for gathering more information about the fate of the SM in the near future. The Tevatron search for the SM Higgs boson will extend its sensitivity to both higher and lower M_H , and then the LHC will enter the game. It is anticipated that the LHC has the sensitivity to extend the Tevatron exclusion down to 127 GeV or less with 1 fb^{-1} of well-understood data at 14 TeV centre-of-mass energy [9]. This would decrease the relative likelihood of the ‘survival’ scenario, but not sufficiently to exclude it with any significance. On the other hand, discovery of a Higgs boson weighing 120 GeV or less would

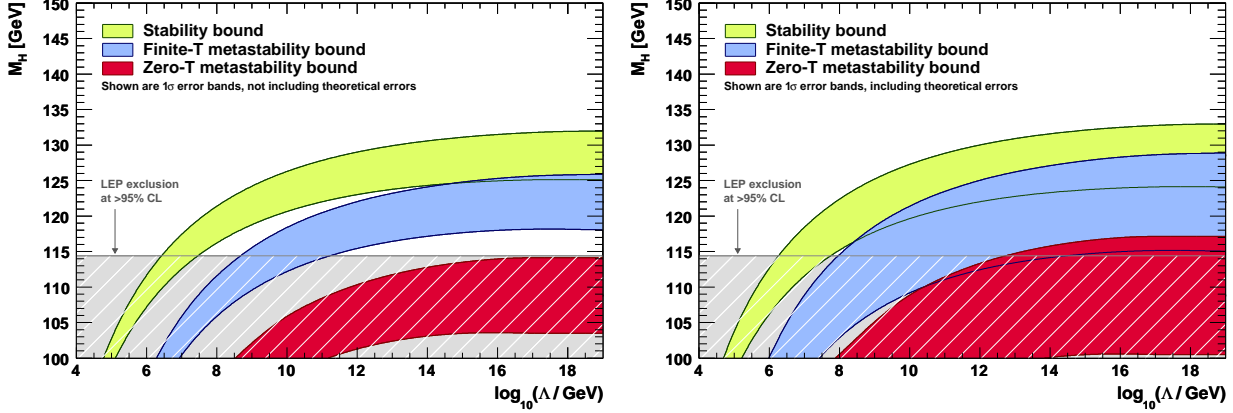


Figure 3: Lower bounds on the Higgs mass due to absolute vacuum stability (light shaded [green]), finite-temperature (medium shaded [blue]) and zero-temperature metastability (dark shaded [red]), as functions of the cut-off scale Λ . The bands indicate the errors induced by the uncertainties in m_t and α_s (added quadratically). The left plot is thus identical to Fig. 2, but with a zoomed ordinate. The right plot includes theoretical uncertainties, which are treated as an offset, i.e., they are not quadratically added to the other errors (cf. Sec 3). At $\Lambda = M_P$, the bounds correspond to Eqs. (4), (6) and (5), respectively.

exclude the ‘survival’ scenario with high significance, implying the presence of a potential instability of the SM at some scale $\Lambda < 10^{10}$ GeV, below the scale for new physics that is suggested by simple seesaw models of neutrino masses.¹

2 Calculation of the SM Higgs Mass Bounds

The SM effective potential for the real Higgs field h can be written in the ‘t Hooft-Landau gauge and the $\overline{\text{MS}}$ renormalisation scheme as $V = V_0 + V_1$, where the tree-level V_0 and one-loop V_1 potentials are given by

$$\begin{aligned}
 V_0 &= -\frac{1}{2}m(\mu)^2 h^2(\mu) + \frac{1}{4}\lambda(\mu)h^4(\mu), \\
 V_1 &= \sum_i \frac{n_i}{64\pi^2} M_i^4(h) \left[\log \frac{M_i^2(h)}{\mu^2} - C_i \right].
 \end{aligned}
 \tag{1}$$

The sum is over all SM particles acquiring a Higgs-dependent mass $M_i(h)$ and having n_i degrees of freedom (taken negative for fermions). The coefficients C_i are $5/6$ ($3/2$) for gauge bosons (scalars and fermions), see Ref. [6] for more details.

Following Ref. [11], we work with the Higgs one-loop effective potential improved by

¹ If the seesaw scale M were higher than $\sim 10^{12}$ GeV the stability and perturbativity bounds would get significantly more stringent above M [10].

two-loop RGEs that resum contributions up to next-to-leading logarithms [12]. The scale independence of the effective potential V allows us to fix the renormalisation scale μ at will for different values of the field [12, 13]. Since our considerations refer to large field values, for our purposes it is appropriate to choose the renormalisation scale to be the value of the Higgs field, and to neglect the bilinear term. The SM Higgs potential is therefore well approximated by

$$V(h) = \frac{\lambda(h)}{4}h^4, \quad (2)$$

where the running quartic coupling absorbs the large logs and includes in its definition a one-loop finite non-logarithmic piece (see Ref. [6] for more details). The quartic Higgs coupling λ and the top-quark Yukawa coupling h_t that enter the RG evolution are related to the physical Higgs and top pole masses through well-known expressions that can be found, *e.g.*, in the Appendix of Ref. [11].

Following Ref. [7], to compute the non-perturbativity bound we define two different conditions for the scale Λ at which we cut off the running: $\lambda_c(\Lambda) = \pi$ and 2π . The first choice, $\lambda_c(\Lambda) = \pi$, corresponds to a two-loop correction to the one-loop beta function β_λ of the Higgs quartic coupling of about 25%, and the perturbative expansion is still meaningful. The second choice, $\lambda_c(\Lambda) = 2\pi$, corresponds to a two-loop correction to β_λ of about 50%. The bold [blue] upper lines in Fig. 2 show the scale Λ at which the two-loop RGEs drive the quartic SM Higgs coupling to the values $\lambda = \pi$ and 2π . The (small) width of the lines represents the errors induced by the uncertainties in m_t and α_s (see below). Values above these lines define the ‘blow-up’ region where, for a given value of the Higgs mass, either there is a scale Λ at which some new non-perturbative dynamics must appear, or there is some scale $< \Lambda$ where new physics appears to avert the blow-up of the Higgs quartic coupling. If we require that this blow-up scale Λ be larger than the reduced Planck scale M_P , so that the SM remains in the perturbative regime, we find

$$M_H < M_H^c + 0.7 \text{ GeV} \left(\frac{m_t - 173.1 \text{ GeV}}{1.3 \text{ GeV}} \right) - 0.4 \text{ GeV} \left(\frac{\alpha_s(M_Z^2) - 0.1193}{0.0028} \right) \pm 1 \text{ GeV} \quad (3)$$

with $M_H^c = 175 \text{ GeV}$ (173 GeV) for $\lambda(M_P) = 2\pi$ (π). We display explicitly the dependencies on the two most important SM parameters, m_t and $\alpha_s(M_Z^2)$, normalising their effects in units of one standard deviation from their experimental central values, for which we use $m_t = 173.1 \text{ GeV} \pm 1.3 \text{ GeV}$ [14] and $\alpha_s(M_Z^2) = 0.1193 \pm 0.0028$ [3] throughout this paper. The third (theoretical) error estimates the uncertainties from higher-order corrections in the running and matching of λ . Figure 4 displays the 1 – CL function at the bound (3) as a narrow ‘pyramid’ representing the uncertain location of the boundary between the stable and non-perturbative regions. The slopes of its sides reflect the uncertainties in m_t and $\alpha_s(M_Z^2)$,

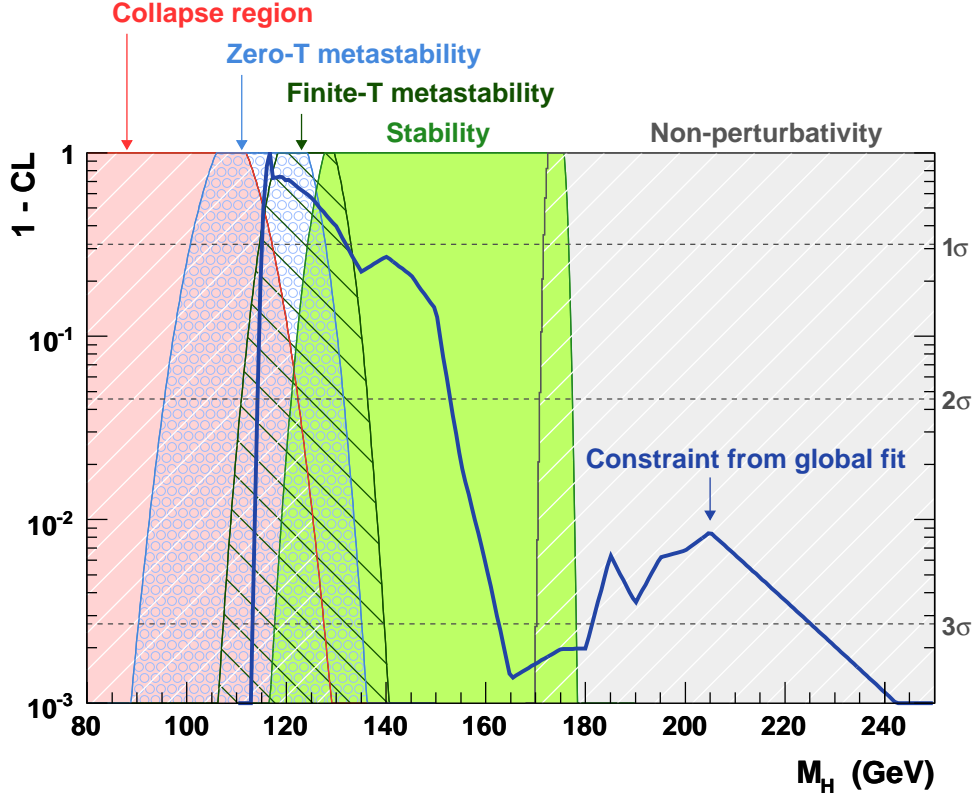


Figure 4: The levels of $1 - CL$ versus M_H for the different scenarios defined by the ultraviolet behaviour of the Higgs potential. The regions are (from left to right): the ‘collapse region’ (light [red] shaded/hatched) corresponding to M_H violating the metastability bound (5) and thus vulnerable to quantum tunneling of the electroweak vacuum in a time shorter than the age of the Universe; the ‘zero-temperature metastability’ region ([blue] dotted) corresponding to values of M_H between the bounds (5) and (4), where quantum tunneling is acceptably slow; the ‘finite-temperature metastability’ region (dark [green] hatched), defined by the lower bound (6), where the local SM minimum is stable against thermal fluctuations up to temperatures equal to M_P ; the ‘stability’ region (darker [green] shaded) delimited by the bounds (4) and (3); and finally the ‘non-perturbativity’ region (light [grey] shaded/hatched), bound by Eq. (3), where the Higgs self-coupling becomes non-perturbative at some scale smaller than M_P . The slopes of the ‘pyramids’ representing the boundaries of the different regions reflect the uncertainties in m_t and $\alpha_s(M_Z^2)$ which lead, together with the theoretical errors affecting the bounds, to apparent overlaps between the regions. Also shown is the $1 - CL$ function for the combination of current constraints on M_H equivalent to the right plot of Fig. 1 (bold solid [blue] line).

and its width at the top reflects the theoretical error, which includes the ambiguity in the choice for $\lambda_c(\Lambda)$. The non-perturbative region at larger M_H is shaded light [grey].

The requirement that the electroweak vacuum be the absolute minimum of the potential, up to a Higgs field scale Λ , implies $\lambda(\mu) > 0$ for any $\mu < \Lambda$. The light shaded [green] band

in Fig. 2 shows the scale Λ at which the RGEs would create a second minimum deeper than the electroweak vacuum ($\lambda < 0$), leading to a possible instability of the SM potential. The width of the band is obtained by varying the top mass and the value of $\alpha_s(M_Z^2)$ by their one-standard-deviation errors. Fig. 3 shows zooms of the low-mass region of Fig. 2: the left plot is identical apart from the change in scale, whereas the right plot includes an estimate of the overall uncertainty due to higher-order corrections. We estimate this uncertainty by adding in the numerical calculation the known, but incomplete, higher-order corrections. The largest effect comes from the two-loop QCD correction to the top-quark pole mass, which amounts to a shift in M_H of about 1 GeV. Since this effect is much larger than the parametric estimate of higher-order corrections, we consider it as a conservative choice for the theoretical error.

Requiring that the SM cannot develop a minimum deeper than the electroweak vacuum for any scale $\Lambda < M_P$, we obtain the following lower bound on the Higgs mass:

$$M_H > 128.6 \text{ GeV} + 2.6 \text{ GeV} \left(\frac{m_t - 173.1 \text{ GeV}}{1.3 \text{ GeV}} \right) - 2.2 \text{ GeV} \left(\frac{\alpha_s(M_Z^2) - 0.1193}{0.0028} \right) \pm 1 \text{ GeV} . \quad (4)$$

The Planck-scale stability bound (4) is also shown in Fig. 4 as a (somewhat broader) 1 – CL ‘pyramid’. Equations (3) and (4) delimit between them the ‘survival’ region (represented as the shaded [green] band in Fig. 4), within which the SM can be safely extrapolated up to the Planck scale.

It should be noted that the ‘unstable’ region is not necessarily incompatible with our existence, as long as the electroweak vacuum survives for a time longer than the age of the universe, before quantum tunneling. The total quantum tunneling probability p throughout the period of the history of the Universe during which thermal fluctuations have been negligible is given by $p = \max_{h < \Lambda} [V_U h^4 \exp(-8\pi^2/3|\lambda(h)|)]$, where $V_U = \tau_U^4$ is the space-time volume of the past light cone of the observable Universe, τ_U being the lifetime of the Universe. Taking $\tau_U = 13.7 \pm 0.2$ Gyrs from the analysis of WMAP data [15] and $p < 1$, one finds that the electroweak vacuum has a sufficiently long lifetime as long as

$$M_H > 108.9 \text{ GeV} + 4.0 \text{ GeV} \left(\frac{m_t - 173.1 \text{ GeV}}{1.3 \text{ GeV}} \right) - 3.5 \text{ GeV} \left(\frac{\alpha_s(M_Z^2) - 0.1193}{0.0028} \right) \pm 3 \text{ GeV} . \quad (5)$$

The error of 3 GeV is estimated by combining uncertainties from higher-order corrections and from the prefactor in p . This constraint is the leftmost ‘pyramid’ in Fig. 4, and the ‘collapse’ region at lower M_H is light [pink] shaded and hatched. The ‘metastability’ bound obtained considering zero-temperature fluctuations up to a scale Λ is plotted as a dark shaded [red] band in Figs. 2 and 3, where the theoretical error is included only in the right plot of the

latter figure. The present LEP lower bound already rules out most of the parameter region where the electroweak vacuum is dangerously unstable, although this hypothesis cannot yet be excluded. We find a p-value of 0.40 for it being compatible with the LEP result.

The ‘metastable’ region above (5) and below (4), although compatible with observations, is rather critical from the cosmological point of view, because the SM vacuum becomes sensitive to thermal or inflationary fluctuations present during the early stages of the Universe [11, 16]. The requirement of thermal metastability depends on the temperature up to which standard Big Bang cosmology is assumed. For instance, requiring the local SM minimum to be stable against thermal fluctuations up to temperatures as large as the Planck scale translates into the lower bound [11]

$$M_H > 122.0 \text{ GeV} + 3.0 \text{ GeV} \left(\frac{m_t - 173.1 \text{ GeV}}{1.3 \text{ GeV}} \right) - 2.3 \text{ GeV} \left(\frac{\alpha_s(M_Z^2) - 0.1193}{0.0028} \right) \pm 3 \text{ GeV} . \quad (6)$$

The $1 - \text{CL}$ function for this constraint is shown as the second ‘pyramid’ from the left in Fig. 4. The ‘finite-temperature metastability’ bound is computed as follows. For fixed M_H in the metastable region there is a calculable maximum temperature that the electroweak minimum can stand without decaying by thermal fluctuations. For temperatures above that maximum value the decay will proceed through thermal nucleation of bubbles that excite the Higgs field at a typical value h_N in the instability region of the effective potential. To prevent this from happening, the effective potential should be modified at or below the scale h_N , which we therefore identify with the cut-off scale Λ corresponding to the metastability bound. (Typically this Λ is one order of magnitude larger than the maximum temperature for thermal tunneling.) The resulting bound is plotted as a medium shaded [blue] band in Figs. 2 and 3, where the theoretical error is included only in the right plot of the latter figure.

Also shown in Fig. 4 is the $1 - \text{CL}$ function for the combined current constraints on M_H [3], equivalent to the right plot of Fig. 1. Both catastrophic scenarios, ‘collapse’ and ‘non-perturbativity’, are disfavoured by the current data, though the former cannot be excluded yet. Numerical results combining the theoretical bounds and available constraint on M_H are given in the following section.

3 Combined Likelihood Analysis

We now convolve the information obtained from the (absolute) stability lower bound and the ‘blow-up’ upper bound on M_H , as functions of Λ , with a likelihood analysis of M_H based on electroweak precision data and the direct Higgs boson searches. The numerical analysis

is performed with the Gfitter package [3]. The latest experimental inputs have been used, including the new world-average top-mass result from the Tevatron [14], a preliminary M_W average [3] incorporating the most recent measurement from the D0 experiment [17], and a new combination of upper limits on production of the SM Higgs boson from the CDF and D0 experiments [2].

The global electroweak fit uses as inputs the masses and widths of the Z and W bosons, the Z hadronic and leptonic decay ratios and forward-backward asymmetries, measurements of the heavy quark masses, and the running fine structure constant at the Z mass. The strong coupling constant $\alpha_s(M_Z^2)$ is determined by the fit. References to all experimental results, their SM predictions and the theoretical uncertainties affecting them are available in Ref. [3]. We include results from the direct Higgs boson searches at LEP [1] as well as the Tevatron [2] in the fit. The statistical procedure follows Ref. [3], where in particular a two-sided CL is used² to estimate the deviation of the measured event yields from the SM hypothesis for given M_H . The floating variables in the global electroweak fit are the coupling strength parameters $\Delta\alpha_{\text{had}}^{(5)}(M_Z^2)$ and $\alpha_s(M_Z^2)$, the Z -boson mass, the quark masses m_t , m_b , m_c , the Higgs boson mass M_H , and four parameters quantifying theoretical uncertainties in the predictions of M_W , $\sin^2\theta_{\text{eff}}^\ell$, and in the form factors absorbing the radiative corrections to the effective weak mixing angle and to the effective vector and axial-vector couplings of the Z boson to fermion-antifermion pairs.

The constraints on M_H from the global fit obtained by the Gfitter Group are shown in Fig. 1, without (left panel) and with (right panel) inputs from the direct Higgs searches in the fit. The 95% CL allowed range for the complete fit (*i.e.*, including the direct searches) is [114, 153] GeV, and above this range only the values between 180 GeV and 224 GeV are not yet excluded at 3 standard deviations or more.

We incorporate the constraints from the (absolute) vacuum stability and perturbativity requirements numerically into Gfitter. In the case of the vacuum stability bound, the dependence on the floating parameters $\alpha_s(M_Z^2)$ and m_t are parametrised linearly and included in the fit. Also included is a universal theoretical error of 1 GeV on the bound, parametrising uncertainties from higher-order perturbative terms (*cf.* Sec. 2). This error, as all theoretical errors in Gfitter, is treated as a fit parameter varying freely within the given range, which corresponds to adding a likelihood term to the fit function that is finite and uniform within this range and zero outside. For the perturbativity bound, we use the more conservative

² The numerical differences in the interpretation of the results from the direct Higgs searches between a one-sided or two-sided CL, or a Bayesian treatment (direct use of the likelihood ratio $\ln Q$), are minor for the present data [3].

choice $\lambda_c(\Lambda) = 2\pi$ (*cf.* Sec. 2). Other theoretical errors are neglected.

The plots in Fig. 5 show the constraints obtained in the two-dimensional plane M_H versus $\log_{10}(\Lambda/\text{GeV})$ from combined fits excluding (upper plot) and including (lower plot) the direct Higgs searches, respectively. The shaded bands indicate the 40% (innermost, darkest), 68%, 95% and 99% (outermost, lightest) CL allowed regions.³ We find that the overall χ^2 estimator has the following minimum values in the planes depicted: 17.2 (excluding the direct Higgs searches) and 17.8 (including the direct searches).⁴ The overall fit is of satisfactory quality for the 13 (14) degrees of freedom excluding (including) the direct Higgs constraint, and we see no need to doubt that the SM is a suitable framework for analysing the available electroweak data (*cf.* the statistical analysis and discussion in Sec. 4.2.3 of Ref. [3]).

The values of M_H favoured by the global fit are compatible with a value of the SM cut-off scale Λ up to the Planck scale. Only for Higgs masses below 124 GeV or above 172 GeV would the bounds provide a constraint on Λ . Because of the small dependence of the stability bound for M_H on Λ , its theoretical uncertainty significantly impacts the value of the constraint obtained.

The Tevatron results do however increase our confidence that, within the SM, the Higgs quartic coupling is perturbative up to M_P . Without the direct Higgs searches, the $\Delta\chi^2$ price is 4.1 for M_H falling into the ‘blow-up’ region, which – assuming a proper χ^2 behaviour – translates into an exclusion of the ‘blow-up’ region at the 95.7% CL. Including the Tevatron Higgs results leads to a higher $\Delta\chi^2$ price of 6.9, corresponding to an improved exclusion at the 99.1% CL. *Hence the SM probably does not blow up before the Planck scale.*

The result of the global fit as a function of Λ can be used to assess the p-value of the ‘survival’ scenario. Figure 6 shows $1 - \text{CL}$ versus Λ for various cases: with and without the theoretical uncertainty in the stability bound, including and excluding the Tevatron Higgs results, and assuming a hypothetical unsuccessful early Higgs search at one of the high- p_T LHC experiments (represented here by ATLAS), for an integrated luminosity of approximately 1 fb^{-1} at 14 TeV centre-of-mass energy, that should have sufficient sensitivity to exclude $M_H > 127\text{ GeV}$ at 95% CL [9].

³ Although the test statistic in Fig. 5 corresponds in principle to two degrees of freedom, an effective constraint on $\log_{10}(\Lambda/\text{GeV})$ only occurs along the bounds, so the number of degrees of freedom in the majority of the plane is one. This is the value we have used to translate the test statistics into the $1 - \text{CL}$ values via $\text{Prob}(\Delta\chi^2, n_{\text{dof}})$. A complete analysis would require the generation of very large numbers of toy Monte Carlo measurements, which is beyond the scope of this paper. (Such a study has been performed in Ref. [3] in the framework of a Two-Higgs-Double Model analysis.)

⁴ The difference in the former number with respect to Ref. [3] (16.4) is due to the restriction to $M_H > 100\text{ GeV}$ and $\Lambda > 10^6\text{ GeV}$ imposed here.

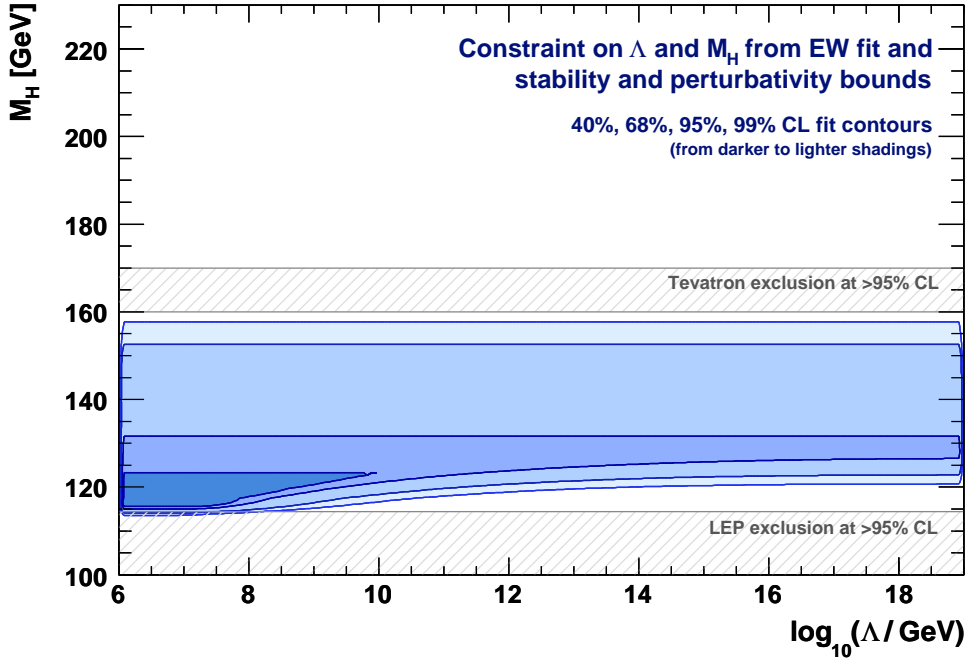
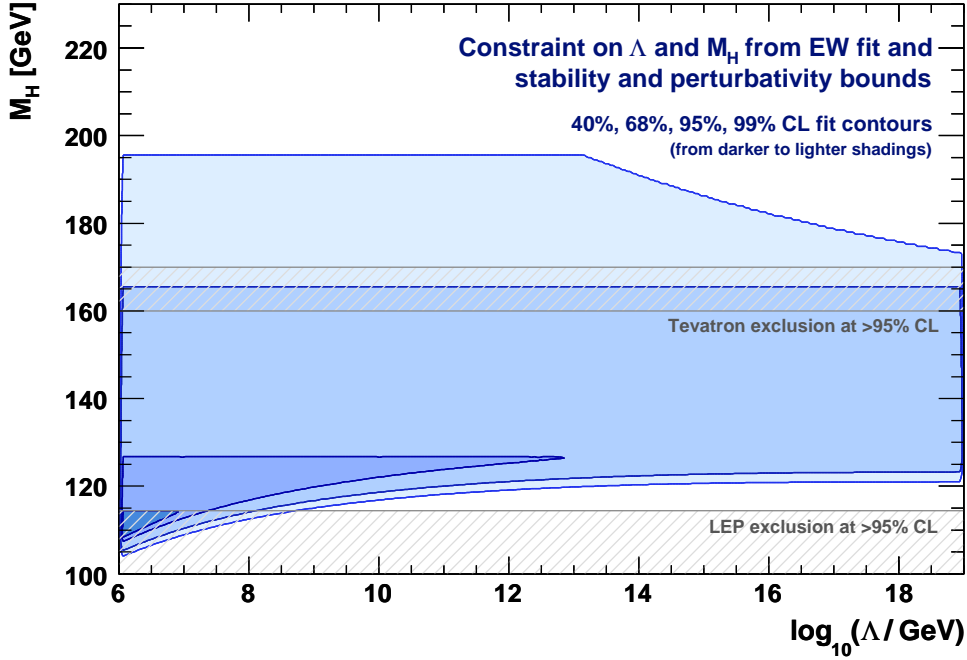


Figure 5: Contours of 40%, 68%, 95% and 99% CL obtained from scans of fits with fixed values of the variables M_H and $\log_{10}(\Lambda/\text{GeV})$. The fits include the electroweak precision data and the bounds from the perturbativity and stability requirements shown in Fig. 2. The lower plot also incorporates the direct Higgs boson searches at LEP and the Tevatron (corresponding to the complete fit scenario in Ref. [3]). Their respective 95% CL exclusion domains are depicted by the hatched bands.

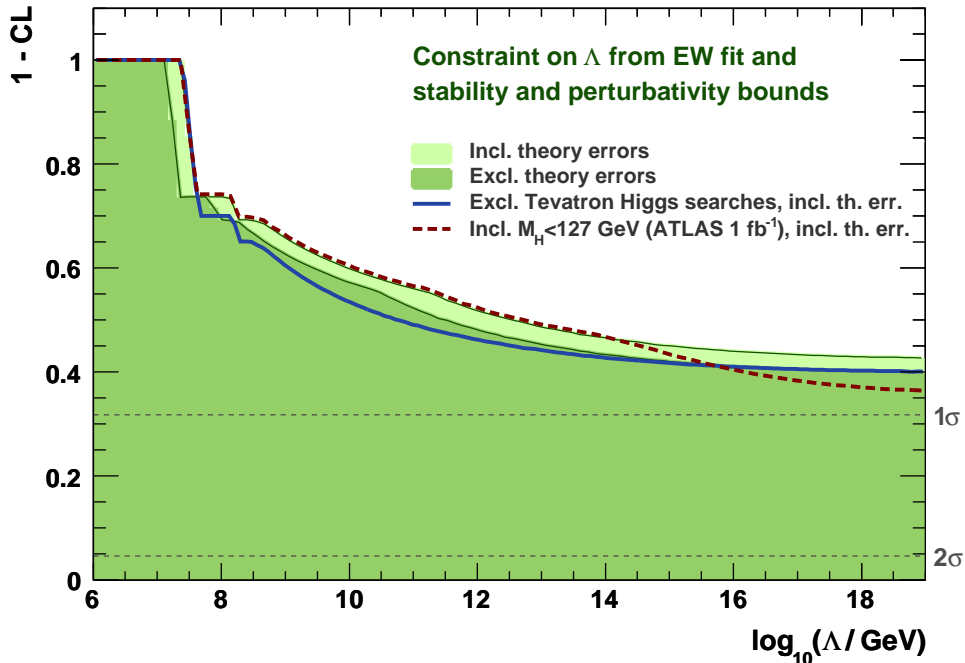


Figure 6: *Constraint on Λ from the global electroweak fit and the requirement of absolute vacuum stability and perturbativity, expressed as $1 - CL$ and assuming it to be given by $Prob(\Delta\chi^2, 1)$. Shown are fits with (light shading) and without (dark shading) taking into account the theoretical uncertainty in the stability bound. The bold solid [blue] line shows the effect of removing the Tevatron Higgs searches from the global fit. The dashed [red] line shows the effect of a hypothetical upper bound of $M_H < 127$ GeV at 95% CL, as might be obtained with early data at the LHC.*

No constraint on Λ (assuming absolute stability) that would reach or exceed 68% CL can be derived from the present data, nor from the prospective incremental improvement in the Higgs constraint that might come from the Tevatron or the early running of the LHC. If, however, there were a Higgs discovery with a mass determined to be $M_H = 120$ GeV or $M_H = 115$ GeV (assumed precision 0.1%) after years of successful LHC operation, one would obtain the constraints on Λ plotted in Fig. 7. For these plots, we have also included prospectives for the precision of the top and W mass measurements of 1 GeV and 15 MeV overall errors, respectively (see references in [3]). The 95% CL upper limits on the cut-off scale obtained including theoretical errors would read $\log_{10}(\Lambda / \text{GeV}) < 10.4$ and 8.0, respectively, including an almost half an order of magnitude theoretical uncertainty. In this case, one would obtain an upper limit on the absolute stability of the SM that would be comparable with the scale suggested by the seesaw model for the light neutrino masses. The p-values of the $M_H = 120$ and 115 GeV scenarios for the ‘survival’ up to M_P are as small as the occurrence of 3.5σ and 5.3σ fluctuations, respectively.

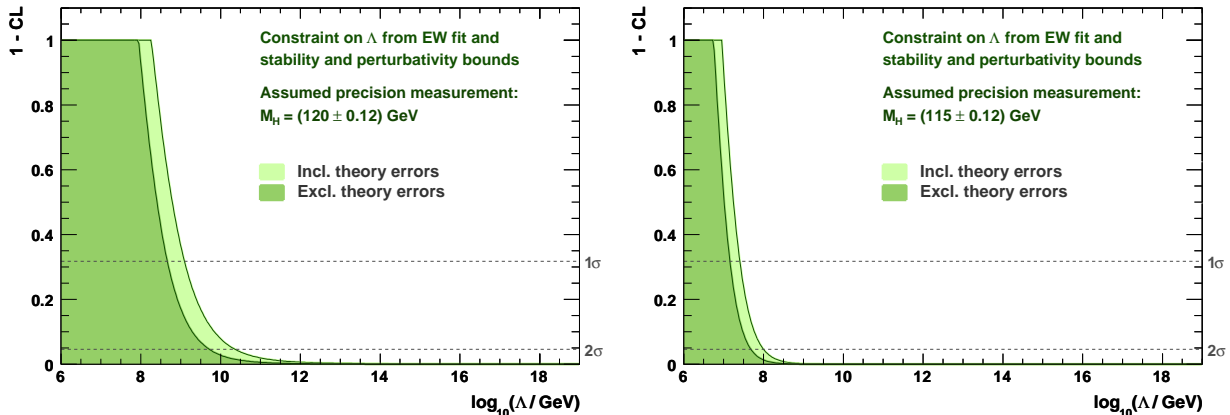


Figure 7: *Constraint on Λ from the global electroweak fit and the requirement of absolute vacuum stability and perturbativity. Included in the fit is a hypothetical Higgs discovery with precise (0.1%) mass measurement at $M_H = 120$ GeV (left plot) and $M_H = 115$ GeV (right plot), respectively. Shown are fits with (light shading) and without (dark shading) taking into account the theoretical uncertainty in the stability bound. Also included are improved errors for the top and W masses, as anticipated for the LHC (see text).*

4 Conclusions

We have combined a global fit of the available electroweak data to the SM and results from direct searches for the SM Higgs boson with theoretical calculations of the effective Higgs potential, using two-loop RGEs to extrapolate its behaviour to high scales. Our analysis displays the impact of the most recent Tevatron searches for an intermediate-mass Higgs boson. We find an exclusion at the 99.1% CL of the possibility that the quartic Higgs coupling of the SM could blow up at some scale Λ below the Planck scale, which the Tevatron data have increased from the 95.7% CL found with the precision electroweak data alone.

On the other hand, the present data exhibit no clear preference between scenarios in which the SM survives up to the Planck scale, and in which it develops new minima at a scale Λ and becomes metastable with respect to either thermal or zero-temperature fluctuations. Here the Tevatron data do not change greatly the *status quo ante* even though they reduce the ‘survival’ region. Nor would a hypothetical LHC upper limit $m_H < 127$ GeV nor, *a fortiori*, hypothetical incremental improvements in the Tevatron upper limit on Higgs production. However, discovery of the Higgs boson might reveal quite conclusively the possible fate of the SM. For example, if the SM Higgs boson were to be discovered with a mass of 120 (115) GeV, the effective potential of the SM would develop a new vacuum at $\log_{10}(\Lambda/\text{GeV}) < 10.4(8.0)$ and remain in a metastable state, unless new physics beyond the SM intervenes. Needless to say, our considerations might be happily irrelevant if LHC finds direct evidence for new

physics at some scale Λ .

Acknowledgements

We are indebted to the Gfitter Group⁵ for making the Gfitter package available, and for the vast collection of experimental results used for the numerical analysis presented in this paper. We also thank Gino Isidori for a useful discussion on metastability bounds. J.R.E. thanks CERN for hospitality and partial financial support. His work is supported in part by CICYT, Spain, under contracts FPA2007-60252; by a Comunidad de Madrid project (P-ESP-00346); and by the European Commission under contracts MRTN-CT-2004-503369 and MRTN-CT-2006-035863.

References

- [1] The ALEPH, DELPHI, L3 and OPAL Collaborations, and LEP Working Group for Higgs Boson Searches, *Phys. Lett. B* **565**, 61 (2003), [hep-ex/0306033].
- [2] Tevatron New Phenomena and Higgs Working Group for the CDF and D0 Collaborations, FERMILAB-PUB-09-060-E, [hep-ex/0903.4001].
- [3] H. Flächer *et al.*, *Eur. Phys. J. C* **60**, 543 (2009) [hep-ph/0811.0009]; updated results taken from <http://cern.ch/gfitter>.
- [4] N. Cabibbo, L. Maiani, G. Parisi and R. Petronzio, *Nucl. Phys. B* **158**, 295 (1979); P. Q. Hung, *Phys. Rev. Lett.* **42**, 873 (1979); M. Lindner, *Z. Phys. C* **31**, 295 (1986); M. Lindner, M. Sher and H. W. Zaglauer, *Phys. Lett. B* **228**, 139 (1989); M. Sher, *Phys. Rept.* **179**, 273 (1989); P. B. Arnold, *Phys. Rev. D* **40** (1989) 613; P. Arnold and S. Vokos, *Phys. Rev. D* **44** (1991) 3620; B. Schrempp and M. Wimmer, *Prog. Part. Nucl. Phys.* **37**, 1 (1996); M. Sher, *Phys. Lett. B* **317**, 159 (1993); G. Altarelli and G. Isidori, *Phys. Lett. B* **337**, 141 (1994).
- [5] G. Isidori, G. Ridolfi and A. Strumia, *Nucl. Phys. B* **609**, 387 (2001), [hep-ph/0104016].
- [6] J. A. Casas, J. R. Espinosa and M. Quirós, *Phys. Lett. B* **342**, 171 (1995), [hep-ph/9409458]; *Phys. Lett. B* **382**, 374 (1996), [hep-ph/9603227]; J. R. Espinosa and M. Quirós, *Phys. Lett. B* **353** (1995) 257 [hep-ph/9504241].

⁵ M. Baak, H. Flächer, M. Goebel, J. Haller, A.H., D. Ludwig, K. Mönig, M. Schott, J. Stelzer.

- [7] T. Hambye and K. Riesselmann, *Phys. Rev. D* **55**, 7255 (1997), [hep-ph/9610272].
- [8] C. F. Kolda and H. Murayama, *JHEP* **0007**, 035 (2000), [hep-ph/0003170].
- [9] ATLAS Collaboration, “Expected Performance of the ATLAS Experiment - Detector, Trigger and Physics”, CERN-OPEN-2008-020, [hep-ex/0901.0512].
- [10] J. A. Casas, V. Di Clemente, A. Ibarra and M. Quirós, *Phys. Rev. D* **62** (2000) 053005 [hep-ph/9904295].
- [11] J. R. Espinosa, G. F. Giudice and A. Riotto, *JCAP* **0805**, 002 (2008), [hep-ph/0710.2484].
- [12] B. M. Kastening, *Phys. Lett. B* **283**, 287 (1992); C. Ford, D. R. T. Jones, P. W. Stephenson and M. B. Einhorn, *Nucl. Phys. B* **395**, 17 (1993); M. Bando, T. Kugo, N. Maekawa and H. Nakano, *Phys. Lett. B* **301**, 83 (1993); M. Bando, T. Kugo, N. Maekawa and H. Nakano, *Prog. Theor. Phys.* **90**, 405 (1993).
- [13] J.A. Casas, J. R. Espinosa, M. Quirós and A. Riotto, *Nucl. Phys. B* **436**, 3 (1995) [Erratum-ibid. B **439**, 466 (1995)], [hep-ph/9407389].
- [14] Tevatron Electroweak Working Group for the CDF and D0 Collaborations, “Combination of CDF and D0 Results on the Mass of the Top Quark,” FERMILAB-TM-2427-E, [hep-ex/0903.2503].
- [15] D. N. Spergel *et al.* [WMAP Collaboration], *Astrophys. J. Suppl.* **170**, 377 (2007), [astro-ph/0603449].
- [16] N. Arkani-Hamed, S. Dubovsky, L. Senatore and G. Villadoro, *JHEP* **0803**, 075 (2008), [hep-ph/0801.2399].
- [17] D0 Collaboration, D0 Note 5893-CONF, 2009.